Proceedings of the ASME 2017 36th International Conference on Ocean, Offshore and Arctic Engineering June 25-30, 2017, Trondheim, Norway

# OMAE2017-62003

# MODELING AND CONTROL OF CRANE OVERLOAD PROTECTION DURING MARINE LIFTING OPERATION BASED ON MODEL PREDICTIVE CONTROL

## Zhengru Ren

Centre for Research-based Innovation Centre for Research-based Innovation Centre for Research-based Innovation on Marine Operations (SFI MOVE) Centre for Autonomous Marine Operations and Systems (AMOS) Department of Marine Technology Norwegian University of Science and Technology, NTNU NO-7491 Trondheim Norway Email: zhengru.ren@ntnu.no

# Roger Skietne

on Marine Operations (SFI MOVE) Centre for Autonomous Marine Operations and Systems (AMOS) Department of Marine Technology Norwegian University of Science and Technology, NTNU Trondheim NO-7491 Norway Email: roger.skjetne@ntnu.no

# **Zhen Gao**

on Marine Operations (SFI MOVE) Centre for Autonomous Marine Operations and Systems (AMOS) Department of Marine Technology Norwegian University of Science and Technology, NTNU Trondheim NO-7491 Norway

Email: zhen.gao@ntnu.no

#### **ABSTRACT**

This paper deals with a nonlinear model predictive control (NMPC) scheme for a winch servo motor to overcome the sudden peak tension in the lifting wire caused by a lumped-mass payload at the beginning of a lifting off or a lowering operation. The crane-wire-payload system is modeled in 3 degrees of freedom with the Newton-Euler approach. Direct multiple shooting and real-time iteration (RTI) scheme are employed to provide feedback control input to the winch servo. Simulations are implemented with MATLAB and CaSADi toolkit. By well tuning the weighting matrices, the NMPC controller can reduce the snatch loads in the lifting wire and the winch loads simultaneously. A comparative study with a PID controller is conducted to verify its performance.

# INTRODUCTION

Due to the oil crisis in 1973-74 and anti-nuclear sentiment, wind farm industry was motivated and started to grow in the late 1970s. At the beginning stage, investment subsidy, tax-free policy, CO<sub>2</sub> bonus, and long-term policy goals stimulated the industry, while it is meanwhile blocked by local protests, siting difficulties, and the inner resistance in the power company [1]. In recent years, there is a significant development of offshore wind farms with an increasing rated power per turbine. Large amounts of newly built offshore wind farms, e.g. in United Kingdom, Denmark, and Germany, have sparked an increasing requirement for safe and cost-and-time efficient installation schemes. Lifting is one of the most common operations during wind turbine installation. Due to the great mass of the payload, sudden wire rope tension at the initial stage of the lifting off and the lowering operation is crucial to the marine installation safety [2]. As largely depending on pragmatic experiences, marine operations ordinarily follow the criteria from guidance documents and confidential data from decades of experience. For example, alpha factor, which is a correction factor on the operational limit in terms of significant wave height, is used to modify the operational criteria and contributes to the decision making process, e.g., when to start a specific operation based on the weather forecasts. To reduce the environmental influence and to provide a stable platform for lifting crane operations, a jackup is the most widely applied scheme. Such methods can merely reduce the risk; however, they are insufficient to satisfy strict deadlines and limitations in operational time windows. The vessel may wait for quite a long period until a calm and long enough weather window for positioning of the jackup rigs. Such operations can only be conducted during the summer time in the North Sea.

Cranes are normally modeled in the framework of Lagrange mechanism by disregarding the axial wire rope elongation. Large amounts of crane models have been developed, for example [3-7]. Hence, a series of basic properties of Lagrange and Hamiltonian system can be applied during the controller design phase [8]. However, the model complexity is unmanageable for those with high degrees of freedom (DOF). In such situation, Newton-Euler modeling method is more straightforward and simpler in the form. For an overhead crane or a ship-mounted onshore situations, the payload is lumped-mass or distributedmass, e.g., [9-11]. To achieve an overall goal of heave compensation through the wave zone during moonpool operations, a number of researches have modeled such process in 1DOF and treat the servo motor as the control input, e.g., [12–15]. However, the model is limited in 1DOF. The main drawback of Newton-Euler model is the difficulty of the model nonlinearities.

Model predictive control (MPC) is widely applied in industry to large multi-variable constrained control problem by solving an online constrained optimization problem repeatedly. Nonlinear model predictive control (NMPC) is an optimal feedback control approach which provides real-time feedback to a nonlinear system through real-time optimizations. An NMPC controller solves a nonlinear dynamic optimization problem at each sampling time. The direct approach performs a discretization for a continuous system on a time grid and solves the programming. It can be categorized into the sequential approach and the simultaneous approach. Direct single shooting method is one of the sequential approaches, and it is unsuitable for longer horizon. Compared to single shooting, the main disadvantages of the simultaneous approach lay on the fact of unnecessary strong nonlinearity of the optimization problem and poor convergence behavior to the desired reference trajectory which may be caused by poor initial guess, especially for unstable system [16]. Due to the limited computational capacity of hardware, online and realtime NMPC is demanding. Real-time iteration (RTI) scheme is an approximation technique for optimal feedback control [17]. The most obvious benefit of RTI scheme is that it performs only one Newton-type iteration per NMPC sample [18].

Automatic code generation is a popular topic due to the requirement for fast solver by the embedded platforms. There exists a group of popular toolboxs with user-friendly interfaces, e.g., CaSADi, ACODO, and CVXGen [19–21]. A number of quadratic programming (QP) solvers which can automatically generate C++ code for the embedded systems have been published, such as FORCES, CVXGen, qpOASES, and FiOrdOs [22,23].

This paper proposes an NMPC control scheme for a winch servo to overcome the sudden tension caused by a lumped-mass payload at the beginning stage of a lifting off or a lowering operation. The paper is structured as follows. In Section 2, the control plant model is proposed. Basic concepts and theories

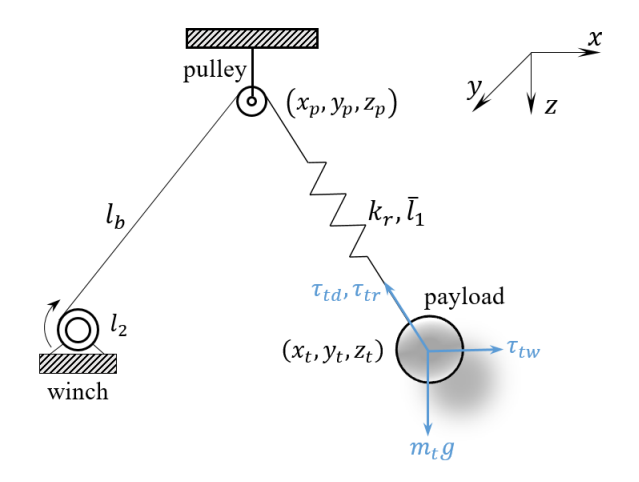


FIGURE 1. FREEBODY DIAGRAM.

about direct multiple shooting approach is introduced in Section 3. Formulation of the optimization problem is shown in Section 4. Simulation studies and discussions are presented in the Sec-

tion 5. Finally, a conclusion summarizes the paper.

**Notation**:  $|\cdot|$  and  $||x||_{\mathcal{Q}}$ , respectively, stand for the Euclidean norm and the weighted Euclidean norm, i.e.,  $|x|^2 = x^T x$  and  $||x||_A^2 = x^T A x$ . The overlines and underlines,  $\underline{\cdot}$  and  $\overline{\cdot}$ , are the lower and upper limits for the variable  $(\cdot)$ . Normal lowercase letters represent scalars. Vectors and matrices are, respectively, expressed with bold lowercase and capital letters.

#### SYSTEM MODELING

A jackup vessel is considered in this paper, and it is assumed to be rigidly fixed on the seafloor. A ship-mounted boom crane on it is responsible for lifting a payload through a wire rope; see Fig. 1. In this paper, we applied a reduced model where the servo motor is the only control input. Hereafter, we consider an infinitely stiff crane, whose position is not influenced by the payload nor the motor. The mass of the payload is  $m_t$ , which is significantly greater than the mass of the rope. Furthermore, we assume a light-weight wire rope, that is, its mass is disregarded. The rope connects to the crane through a pulley at the crane tip. We assume the position of the wire tangency point coincides with the center of the pulley, and its relative position to the boom is fixed. Therefore, the rope and the hook are modeled as a tensile spring. The length of the unstretched wire rope between the pulley and the payload is  $\bar{l}_1$ . The mass of the hook is combined into the payload, which does not interact with the water surface. Only the wind load is included.

Inspired by the finite element method model, a lifting model with elastic wire rope and controllable winch is deduced in the perspective of the Newton-Euler method. The system is modeled

in the 3DOF (NED) frame, and it has a relatively simple form, when comparing with the Euler-Lagrange approach. The positive directions of the coordinate point are to the north, the east, and downward, respectively. Now, define the following vectors:

the position of the payload:  $\mathbf{r}_t = [x_t, y_t, z_t]^{\top},$  the position of the pulley:  $\mathbf{r}_p = [x_p, y_p, z_p]^{\top},$  the velocity of the payload:  $\mathbf{u}_t = [\dot{x}_t, \dot{y}_t, \dot{z}_t]^{\top},$  the velocity of the pulley:  $\mathbf{u}_p = [\dot{x}_p, \dot{y}_p, \dot{z}_p]^{\top},$ 

where the subscripts t and p represent the payload and the pulley, respectively. In this paper,  $\mathbf{u}_p = [0,0,0]^{\top}$  as we assume both the jackup and the crane are rigidly fixed.

We define two additional vectors to simplify the following expressions. Position vector from the pulley to payload and its time derivative are defined as

$$\boldsymbol{\Delta}_1 := \boldsymbol{r}_t - \boldsymbol{r}_p, \tag{1a}$$

$$\Delta_2 := \boldsymbol{u}_t - \boldsymbol{u}_p. \tag{1b}$$

Based on the Newton's second law, the sum force of the payload is the sum of gravity  $\boldsymbol{G}$ , restoring force  $\boldsymbol{\tau}_{tr}$ , the damping  $\boldsymbol{\tau}_{td}$ , and wind load  $\boldsymbol{\tau}_{tw}$ , i.e.,

$$\mathbf{M}_{t}\dot{\mathbf{u}}_{t} = \mathbf{G} + \mathbf{\tau}_{tr} + \mathbf{\tau}_{td} + \mathbf{\tau}_{tw}. \tag{2}$$

#### Restoring force

The restoring force is modeled as a tensile spring which only reacts when the axial elongation is positive, i.e.,

$$\boldsymbol{\tau}_{tr} = -\kappa(\delta)k_r \delta \frac{\boldsymbol{\Delta}_1}{|\boldsymbol{\Delta}_1|}, \quad \kappa(\delta) = \begin{cases} 1 & \delta \ge 0, \\ 0 & otherwise, \end{cases}$$
 (3)

where the restoring acting coefficient is  $\kappa$ , and the axial elongation is

$$\delta = |\mathbf{\Delta}_1| - \bar{l}_1,\tag{4}$$

where  $\frac{|\Delta_1|}{\Delta_1}$  is responsible for dividing the total force into three components in the NED frame, and the elastic stiffness of the lifting wire rope  $k_r$  is a function of its length, as well as the

the characteristics of the wire rope, e.g., material, diameter, and strand construction. For simplification, we consider the rope between the pulley and the hook and the rope between the hook and payload as a whole. That is, the generalized stiffness is modeled as.

$$k_r = \gamma \frac{EA_r}{l_1},\tag{5}$$

where E denotes the Young's modulus,  $A_r$  refers to the cross-sectional area of the rope, and  $l_1 = \overline{l_1} + l_b$ , where  $l_b$  is the length of rope between the winch and pulley, which is assumed to be a constant. A general form for the modified coefficient for a stranded wire is deduced in [24], given by

$$\gamma = \sum_{i=0}^{n} \frac{z_i \cos^3 \alpha_i}{1 + v_i \sin^2 \alpha_i} E_i A_{ri}, \tag{6}$$

where *n* is the number of wire layers counted from the inside with i=0 for the center wire, and  $E_i$ ,  $A_{ri}$ ,  $\alpha_i$ , and  $v_i$  are the Young's modulus, the cross-sectional area, the lay angle, and the Poisson ratio of a wire in the the  $i^{th}$  wire layer, respectively. A specific example of Eqn. (6) is  $\gamma = \frac{\cos^3 \alpha}{1 + v \sin^2 \alpha}$  when all the strands share a same lay angle and Poisson ratio.

# **Damping**

A ship-mounted crane normally is lightly damped. The damping ratio is, approximately, 0.1-0.5% of the critical damping [25]. The damping force is given by

$$\boldsymbol{\tau}_{td} = -d_l \dot{\boldsymbol{\delta}} \frac{\boldsymbol{\Delta}_1}{|\boldsymbol{\Delta}_1|} = -\frac{d_l}{|\boldsymbol{\Delta}_1|} (\frac{\boldsymbol{\Delta}_1^{\top} \boldsymbol{\Delta}_2}{|\boldsymbol{\Delta}_1|} - v_1) \boldsymbol{\Delta}_1, \tag{7}$$

where  $v_1 = \dot{l}_1$  is the winch speed,  $d_l$  is the damping coefficient and the changing rate of elongation  $\dot{\delta}$  is deduced from Eqn. (4), that is,

$$\dot{\delta} = \frac{\mathbf{\Delta}_1^{\top}}{|\mathbf{\Delta}_1|} \mathbf{\Delta}_2 - v_1. \tag{8}$$

The above simplification is based on the fact that  $\mathbf{\Delta}_1^{\top}\mathbf{\Delta}_1 = |\mathbf{\Delta}_1|^2$ .

#### Wind load

When the payload is a lumped mass, or a rigid-point, the wind load is small compared to the other force components. Morison equation is used to calculate the wind load, which is given by

$$\boldsymbol{\tau}_{tw} = -\frac{1}{2}\rho C_d A_t \left(\boldsymbol{u}_t - \boldsymbol{v}_w(z)\right) \left|\boldsymbol{u}_t - \boldsymbol{v}_w(z)\right|, \tag{9}$$

where  $A_t$  is the reference cross-sectional area of the payload perpendicular to the wind direction,  $v_w(z) \in \mathbb{R}^3$  is the wind speed at the corresponding height. Henceforward, we only consider the horizontal winds and disregard the vertical component, due to its small magnitude, s.t.,  $\mathbf{v}_w(z) = [U_w(z)\cos\alpha_w, U_w(z)\sin\alpha_w, 0]^\top$ , where  $\alpha_w$  is the wind angle at the corresponding height, and the wind speed  $U_w(z)$  is a sum of the mean component, the slowly-varying component, and the wind gust. See [26] for more details.

## Model summary

Substitute Eqn. (3), Eqn. (7), and Eqn. (9) into the Newton's second law (2). Based on the assumptions that the elongation is constantly semi-positive, i.e.,  $|\Delta_1| \ge \bar{l}_1$ , the control plant model is given by

$$\dot{\boldsymbol{r}}_t = \boldsymbol{u}_t, \tag{10a}$$

$$\boldsymbol{M}_{t}\dot{\boldsymbol{u}}_{t} = -\boldsymbol{A}(\boldsymbol{r}_{t}, \boldsymbol{r}_{\boldsymbol{p}}, l_{1}, v_{1})\boldsymbol{\Delta}_{1} + \boldsymbol{G} + \boldsymbol{\tau}_{tw}, \tag{10b}$$

$$\dot{l}_1 = v_1, \tag{10c}$$

$$\dot{v}_1 = u,\tag{10d}$$

where the mass matrix  $\mathbf{M}_t = \operatorname{diag}(m_t, m_t, m_t), \mathbf{A}(\mathbf{r}_t, \mathbf{r}_p, l_1, v_1) \in \mathbb{R}^{3 \times 3}$  is the diagonal matrix,  $\mathbf{A} = \operatorname{diag}\{a_t, a_t, a_t\}$ , with  $a_t = \gamma E A \frac{|\mathbf{\Delta}_1| - \bar{l}_1}{\bar{l}_1 |\mathbf{\Delta}_1|} + \frac{d_l}{|\mathbf{\Delta}_1|} (\frac{\mathbf{\Delta}_1^{\top} \mathbf{\Delta}_2}{|\mathbf{\Delta}_1|} - v_1)$ , and  $\mathbf{G} = [0, 0, m_t g]^{\top}$  is the gravity. The nonlinearity in the differential equations (10) mainly comes from term  $a_t$ .

### **DIRECT MULTIPLE SHOOTING**

Optimization is a process to find the reasonable inputs for some nonlinear functions to ensure the system outputs satisfy the desired performance. Direct method is applied to transform the continuous system with infinite dimensions to a discrete nonlinear programming question with finite dimensions. In this paper, the direct multiple shooting approach is adopted for discretization and numerical integrator for prediction.

Originally proposed in [27], direct multiple shooting method transforms a continuous optimal control problem into a nonlinear

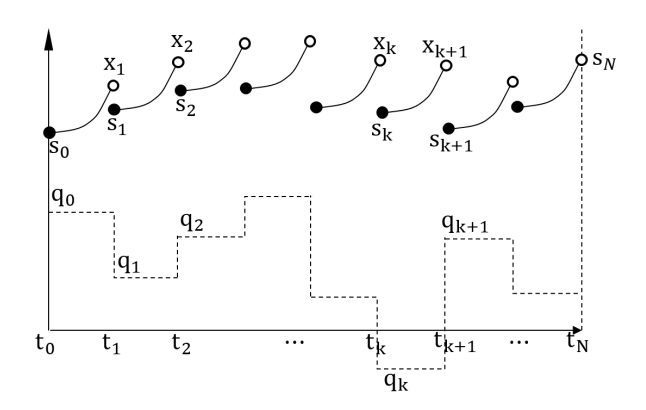


**FIGURE 2.** ILLUSTRATION OF DIRECT MULTIPLE SHOOTING.

programming problem based on the discretization of state variables and control inputs and finite dimensional parameterization of the path constrains. The state variables and control inputs are approximated by shooting nodes and piecewise functions. After that, the problem is solved by a quasi-Newton method.

A time horizon  $[t_0, t_0 + T]$  is partitioned into N subintervals. Normally, the length of a subinterval equals to the sampling time. A fixed step size  $\delta t = T/N$  is applied, for simplification. To simplify the expression,  $x(t_k)$  is written as  $x_k$ , where  $t_k = t_0 + k\delta t$ . Then, a time grid is achieved, i.e.,  $t_0 < t_1 < \cdots < t_N$ .

For one specific subinterval  $[t_k, t_{k+1}]$ ,  $x(t_{k+1}) = F(x_k, u_k)$ , where F is an explicit integrator, which approximates the solution mapping numerically. Two extra terms,  $s_i$  and  $q_i$ , are introduced to avoid confusions with real system states x and u, i.e.,  $s_{k+1} = F_k(s_k, q_k)$ . Here, the zero-order hold signal is employed as the resulting control input function to form a finite-dimensional nonlinear programming problem, i.e.,  $u(t;q) = q_k$  is a constant variable in one time horizon  $\forall t \in [t_k, t_{k+1}]$ . The notations of above mentioned parameters are illustrated in Fig. 2.

A constrained least-square dynamic optimization problem of multiple shooting is given by

$$\min_{S,Q} \frac{1}{2} \sum_{k=0}^{N-1} l_k(s_k, q_k) + E(s_N), \tag{11a}$$

s.t. 
$$x_0 - s_0 = 0$$
, (11b)

$$F(t_{k+1}; t_k, s_k, q_k) - s_{k+1} = 0, \quad k = 0, \dots, N-1,$$
 (11c)

$$h(s_k, q_k) \le 0, \qquad k = 0, \dots, N, \tag{11d}$$

$$r(s_N) \le 0, \tag{11e}$$

where  $S = [s_1, \dots, s_N]$  denotes the state trajectory,  $Q = [q_1, \dots, q_{N-1}]$  refers to the control trajectory.,  $x_k$  is the states at the  $k^{th}$  time interval, Eqn. (11b) is the initial value, Eqn. (11c)

denotes the continuity condition, Eqn. (11d) specifies the path constraints, and Eqn. (11e) gives the terminal constraints. The objective function can be chosen as, for example,

$$l_k(s_k, q_k) = \left( \|s_k - x_k^{ref}\|_{\mathscr{Q}}^2 + \|q_k - u_k^{ref}\|_{\mathscr{R}}^2 \right),$$
  
$$E(s_N) = \|s_N - x_N^{ref}\|_{\mathscr{P}}^2,$$

where  $\mathcal{Q}, \mathcal{R}$ , and  $\mathcal{P}$  are positive-definite diagonal weighting matrices.

Path constraints, for instant, can be selected in the following form:

$$\underline{u} \le u_k \le \overline{u},$$
  $k = 0, \dots, N-1,$   
 $\underline{x} \le s_k \le \overline{x},$   $k = 0, \dots, N-1,$ 

where  $\underline{s}$ ,  $\overline{s}$  and  $\underline{u}$ ,  $\overline{u}$  are determined by the operational criteria and system limitations. The superscript ref means reference signal. The continuity condition must be satisfied, shown in Eqn. (11c). The NLP problem can be solved by an established NLP solver, for example, ipopt [28]. See [29] and [30] for more details.

# PROBLEM FORMULATION Motivation example

At the beginning of the simulations, the payload is hanging at an equilibrium point, where there is no axial oscillation in the wire. If a sudden lifting off or lowering operation with a constant lifting speed is executed at 0.5 seconds, the wire tension history is shown in Fig. 3 and Fig. 4. Slash loads or sudden peak tensions are excitated, followed by underdamped oscillations due to the axial damping. In the figures, the changing parameters are the payload's mass and the lifting speed. From the simulation results, we notice that a large sudden tension happens at the beginning of the lifting operation. The magnitude of tension oscillation increases with both the payload mass and the speed. The lifting speed does not influence the natural frequency of the crane-wire-payload system. The heavier the payload is, the lower the nature frequency will be. This is similar to a basic mass-damper-spring system, i.e.,  $m_t \ddot{z}_t + k_r z_t = m_t g$ , then the natural frequency is  $\omega_n = \sqrt{\frac{k_r}{m_t}}$ . From Eqn. (5), the restoring coefficient  $k_r$  increases when the wire length reduces. The tension variance caused by the payload's horizontal motion is negligible when comparing with the sudden tension. The axial oscillation amplitude reduces slowly due to the low axial damping ratio.

Jerks happen easier with lighter payload and higher lifting speed. Snatch loads are aroused during this process, which may potentially break the wire. Thus, the minimum value for the axial

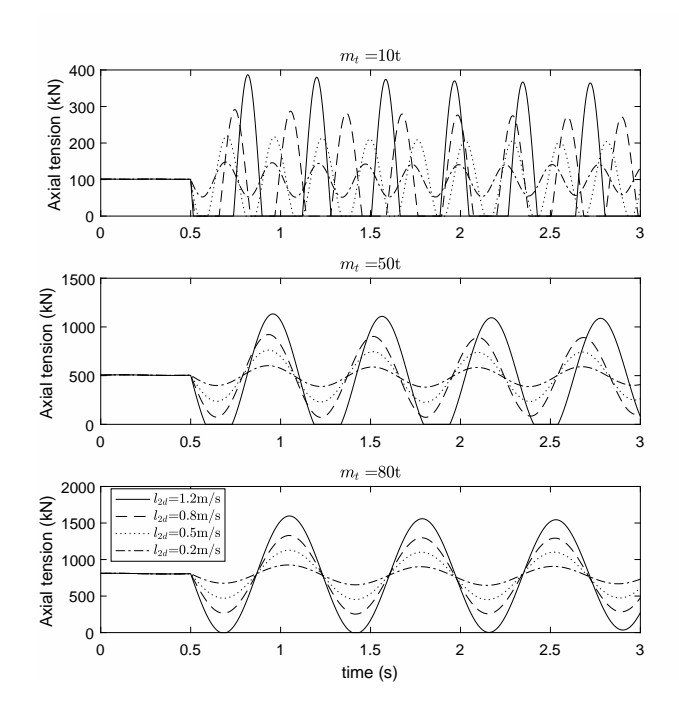


**FIGURE 3**. THE AXIAL TENSION OF THE WIRE ROPE WITH A CONSTANT LIFTING OFF SPEED.

tension of the wire should never be less than zero. When snatch loads appear in the tension history, it is easy to notice that the interval between the snatch starting and ending point is longer than the oscillation period. This is because the restoring force no longer acts on the payload when  $\delta < 0$ .

This paper proposes a control algorithm to achieve improved lifting performance. The primary control objectives are listed as follows:

- (a) Reach the desired lifting speed  $v_{1d}$  in a minimum time;
- (b) Protect the overload tension during the lifting operation by controlling the winch speed;
- (c) Avoid jerks and snatch loads;
- (d) Avoid winch servo motor burnout by limiting the winch maximum acceleration;
- (e) Limit the winch servo motor's maximum speed;
- (f) Reduce the wear-and-tear effects on the wire rope.

# NMPC problem formulation

For the aforementioned lifting question, the nonlinear programming problem is given by

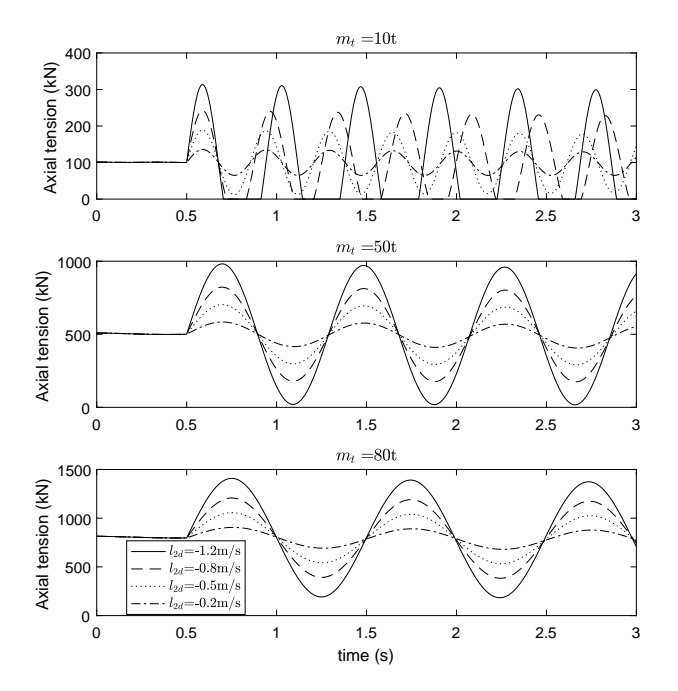


FIGURE 4. THE AXIAL TENSION OF THE WIRE ROPE WITH A CONSTANT LOWERING SPEED.

$$\min_{S,Q} \sum_{k=0}^{N} \left[ k_{\delta} \left( \frac{d}{dt} |\Delta_{1}| - v_{1} \right)^{2} + k_{d} (v_{1} - v_{1d})^{2} \right] + \sum_{k=0}^{N-1} k_{u} u^{2}, \quad (12a)$$
s.t.  $\underline{u} \le u \le \overline{u}, \qquad k = 0, \dots, N-1, \quad (12b)$ 

$$|\Delta_{1}| - \overline{l_{1}} \le 0, \qquad k = 0, \dots, N, \quad (12c)$$

$$|\dot{\Delta}|_{1} - v_{1d} = 0, \qquad k = N. \quad (12d)$$

s.t. 
$$\underline{u} \le u \le \overline{u}$$
,  $k = 0, \dots, N-1$ , (12b)

$$|\Delta_1| - l_1 \le 0, \qquad k = 0, \dots, N, \tag{12c}$$

$$|\dot{\mathbf{\Delta}}|_1 - v_{1d} = 0, \qquad k = N. \tag{12d}$$

where  $\frac{d}{dt}|\mathbf{\Delta}_1| = \frac{\mathbf{\Delta}_1^{\top}\mathbf{\Delta}_2}{|\mathbf{\Delta}_1|}$ ,  $k_u$ ,  $k_{\delta}$ , and  $k_d$  are the weights. During the modeling process, the wind load is disregarded, due to its low magnitude when comparing with the payload's gravity. There are eight states, one control input, and 20 or 40 prediction intervals in the problem. The objective function is about the axial restoring force changing rate, the lifting speed error, and the control input. The computational efficiency largely depends on the initial guess.

The objective function (12a) depicts the difference between the real-time lifting speed and the winch speed, the difference between the winch speed and the desired lifting speed, and the cost of winch input. The first term aims to limit the axial elongation and protect the overload tension. The second term ensure the desired lifting speed is reached in a minimum time. The inequality constraint (12b) intends to avoid winch servo motor burnout caused by extremely large winch speed acceleration. The boundary values, u and  $\overline{u}$ , are determined by the winch's physical configuration. The inequality constraint (12c) is used to avoid snatch

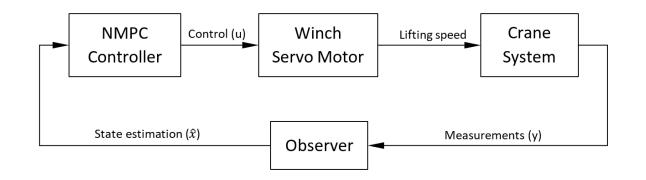


FIGURE 5. BLOCK DIAGRAM OF THE NMPC CONTROLLER.

loads by avoiding the elongation always not negative. The equality constraint (12d) guarantees that the lifting speed meets the preseted value at the terminal time instant.

RTI and shifting schemes are applied to accelerate the calculations. Both of them can increase the computation speed in the real-time application. The main strategy for the real-time iteration is to perform only once sequential quadratic programming per sampling time. See [16] for details. A shifting scheme is applied to construct the initial guess for the next sampling interval [31]. We assume that the states are fully observable and an observer has already filtered the sensor noises; see Fig. 5. It is also reasonable to assume the payload's motion in the horizontal plane is bounded.

# SIMULATION AND RESULTS Simulation overview

The simulation is conducted in MATLAB environment. CaSADi with MATLAB interface is selected to model and solve the nonlinear programming problem. The solver is ipopt. There are two scenarios in the simulations:

- (a) Scenario I: Start a lifting off operation, with an initial speed  $v_1(0) = 0m/s$  and a desired speed  $v_{1d} = 1.2m/s$ ;
- (b) Scenario II: Start a lowering operation, with an initial speed  $v_1(0) = 0m/s$  and a desired speed  $v_{1d} = -1.2m/s$ .

The system parameters are tabulated in Tab. 1. In the simulations, the mass of the payload is chosen as 50 tons. The control horizon is 2 seconds with 40 subintervals.

To compare the performance of the NMPC controller with traditional PID controllers, a simple P controller, where  $k_p = 2$ , is given by

$$\dot{v}_1 = -k_p(v_1 - v_{1d}). \tag{13}$$

The P controller accelerates the winch to the desired value without any feedback from the plant model.

# Simulation results

After tuning the weight matrices in the objective function in (12a), the performance is shown in Fig. 6-9. The P-controller is

**TABLE 1**. PARAMETERS OF THE PAYLOAD AND THE WIRE ROPE.

Parameter	Symbol	Unit	Value
Mass of the payload	$m_t$	ton	50
Initial suspended rope length	$\bar{l}_1(0)$	m	10
Length of rope at the boom	$l_b$	m	60
Elastic module	$\gamma EA$	N	$1.05\times10^9$
Initial lifting speed	$l_2(0)$	$\frac{m}{s}$	0
Desired lifting speed	$v_{1d}$	$\frac{m}{s}$	$\pm 1.2$
Winch speed boundary	$[\underline{\nu}_1,\overline{\nu}_1]$	$\frac{m}{s}$	[-2, 2]
Winch acceleration boundary	$[\underline{u},\overline{u}]$	$\frac{m}{s^2}$	[-2, 2]

included in Fig. 7 and Fig. 9.

In Scenario I, we notice that the lift speed reaches the desired speed within 2 seconds, both with the P-controller and the NMPC controller. However, the P-controller gives a more smooth control input profile, while the axial oscillation cannot be removed. Because of the low damping ratio of the wire rope, the rope keeps oscillating after the lifting speed reaches the desired value. Furthermore, it is easy to notice that the NMPC controller reaches the desired lifting speed without oscillation.

The winch accelerates with its upper limited acceleration, at the beginning stage  $(0-0.45\,s)$ . Then it starts to reduce the acceleration to achieve the desired lifting speed, approximately at  $0.7\,s$ . The lifting speed reaches the desired value quickly, with a quite small overshoot. The winch controller still changes the control input after reaching to the desired control objective. There are several reasons for this. First of all, due to the overshoot in the lifting speed control. Secondly, the payload motion in the horizontal x-y plane can, but only slightly, influence the axial tension. We have noticed that the axial tension is well bounded, and it stabilizes at  $1.5\,s$ . After that, the tension still oscillates with a low frequency and magnitude caused by the horizontal motion.

In Scenario II, the results are similar to Scenario I. Comparing to the P-controller, the NMPC controller shows a better capacity to limit the axial oscillation. Therefore, NMPC controller can reduce the wear-and-tear effect in the wire.

# **Discussion**

We have experienced that the controller has poor performance when the sample interval becomes larger than the system natural period. This is because the NMPC controller optimizes the feedback control based on the discretized states. In this situation, the Nyquist-Shannon sampling theorem is not satisfied,

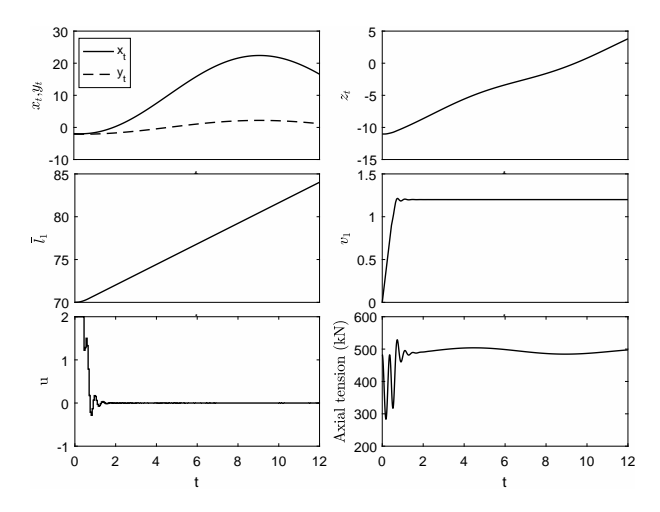


**FIGURE 6**. SIMULATION RESULTS OF THE NMPC CONTROLLER, SCENARIO I.

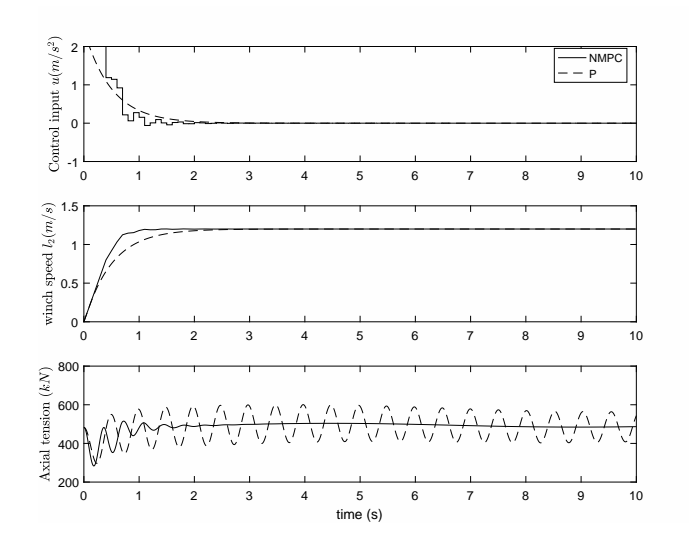


**FIGURE 7.** SIMULATION RESULTS BETWEEN THE NMPC CONTROLLER AND THE P CONTROLLER. SCENARIO I.

i.e., the discrete signals do no longer represent the continuous responses. The performance is improved with smaller sampling and control intervals, since the controller then will have a more subtle control. However, the sampling interval is limited by the embedded hardware and its computational capability. Therefore, a balance must be found.

The difference in performance for various time horizons is quite small. This is because the natural frequency of the wire rope is much smaller than the optimal horizon. Therefore, several tension oscillation periods happen even within a short horizon, e.g., 2 seconds.

The weights in the cost function determine the control emphasis, to reduce the wear-and-tear effects or to maximize the

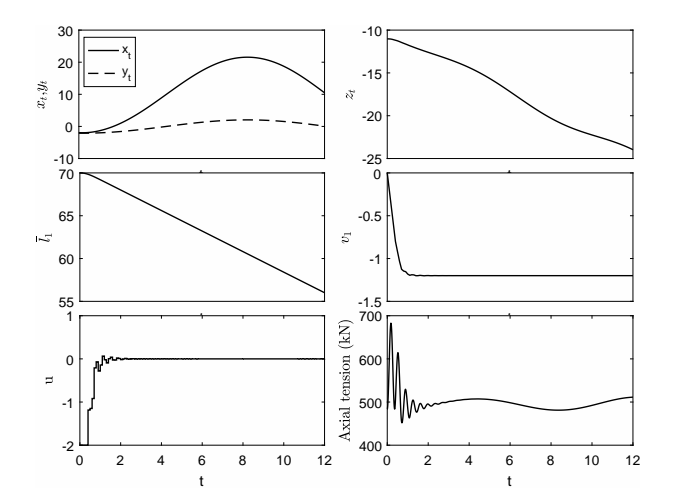


**FIGURE 8**. SIMULATION RESULTS OF THE NMPC CONTROLLER, SCENARIO II.

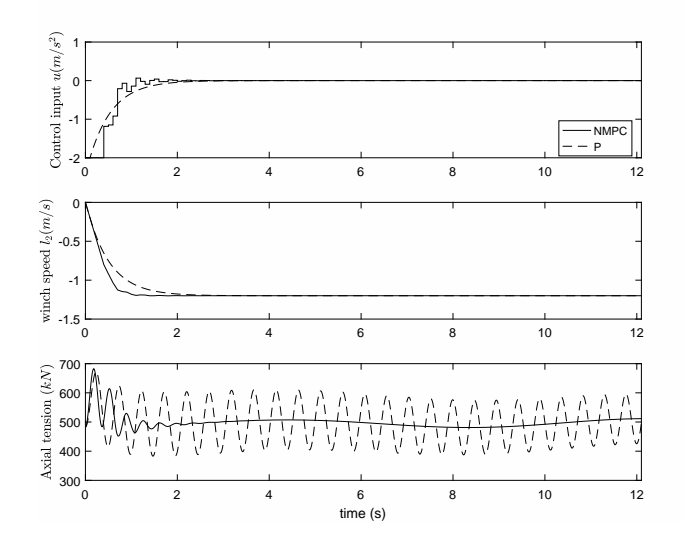


**FIGURE 9**. SIMULATION RESULTS BETWEEN THE NMPC CONTROLLER AND THE P CONTROLLER, SCENARIO II.

control performance. The gain value for the end step is less important than the gains in the Mayer term. This is because this weight only determines one value among N+1 values in the sum operator. However, we can prioritize the final performance by increasing it.

Based on the simulation results, the direct single shooting is much faster than the direct multiple shooting approach. This is because the number of KKT conditions in a single shooting is much smaller than those of multiple shooting. However, its strong dependency on the initial guess limits its application.

#### CONCLUSION

In this paper, an NMPC controller is introduced to limit the sudden overload at the beginning of a lifting or lowering operation. The control plant model is modeled in the Newton-Euler approach. Based on the simulation results, the NMPC controller can efficiently limit the sudden tension and reduce the wear-and-tear effects.

Further study will focus on the robust optimal control, for example, tube-based model predictive control. The objective is further to ensure that the system still performs well when exposed to strong winds. Additionally, more complex distributed-mass payload will be studied.

### **ACKNOWLEDGMENT**

This work was supported by the Research Council of Norway (RCN) through the Centre for Research-based Innovation on Marine Operations (RCN-project 237929), and partly by the Centre of Excellence AMOS (RCN-project 223254).

#### **REFERENCES**

- [1] Buen, J., 2006. "Danish and norwegian wind industry: The relationship between policy instruments, innovation and diffusion". *Energy Policy*, *34*(18), pp. 3887 3897.
- [2] Zhao, Y., Gao, Z., Moan, T., and Sandvik, P. C., 2016. "Study on lift-off of offshore wind turbine components from a barge deck with emphasis on snathch load in crane wire". In Marine Operations Specialty Symp., pp. 249–265.
- [3] Abdel-Rahman, E. M., Nayfeh, A. H., and Masoud, Z. N., 2003. "Dynamics and control of cranes: A review". *J. Vibration and Control*, **9**(7), pp. 863–908.
- [4] Spathopoulos, M., and Fragopoulos, D., 2004. "Pendulation control of an offshore crane". *Int. J. of Control*, **77**(7), pp. 654–670.
- [5] Masoud, Z., Nayfeh, A., and Mook, D., 2004. "Cargo pendulation reduction of ship-mounted cranes". *Nonlinear Dynamics*, **35**(3), pp. 299–311.
- [6] Chin, C.-M., Nayfeh, A. H., and Mook, D. T., 2001. "Dynamics and control of ship-mounted cranes". *J. Vibration and Control*, 7(6), pp. 891–904.
- [7] Chin, C., Nayfeh, A., and Abdel-Rahman, E., 2001. "Non-linear dynamics of a boom crane". *J. Vibration and Control*, 7(2), pp. 199–220.
- [8] Olfati-Saber, R., 2001. "Nonlinear control of underactuated mechanical systems with application to robotics and aerospace vehicles". PhD thesis, Cambridge, MA, USA. AAI0803036.
- [9] d'Andréa Novel, B., and Coron, J.-M., 2000. "Exponential stabilization of an overhead crane with flexible cable via a back-stepping approach". *Automatica*, *36*(4), pp. 587–593.

- [10] Sun, N., Fang, Y., and Zhang, X., 2013. "Energy coupling output feedback control of 4-dof underactuated cranes with saturated inputs". *Automatica*, **49**(5), pp. 1318–1325.
- [11] Tang, R., and Huang, J., 2016. "Control of bridge cranes with distributed-mass payloads under windy conditions". *Mech. Systems and Signal Proc.*, 72, pp. 409–419.
- [12] Sagatun, S. I., Johansen, T. A., Fossen, T. I., and Nielsen, F. G., 2002. "Wave synchronizing crane control during water entry in offshore moonpool operations". In Control Applications, 2002. Proc. of the 2002 Int. Conf. on, Vol. 1, IEEE, pp. 174–179.
- [13] Johansen, T. A., Fossen, T. I., Sagatun, S. I., and Nielsen, F. G., 2003. "Wave synchronizing crane control during water entry in offshore moonpool operations-experimental results". *IEEE J. Oceanic Eng.*, **28**(4), pp. 720–728.
- [14] Skaare, B., and Egeland, O., 2006. "Parallel force/position crane control in marine operations". *IEEE J. Oceanic Eng.*, 31(3), pp. 599–613.
- [15] Messineo, S., and Serrani, A., 2009. "Offshore crane control based on adaptive external models". *Automatica*, **45**(11), pp. 2546–2556.
- [16] Diehl, M., Findeisen, R., Allgower, F., Bock, H. G., and Schloder, J., 2003. "Nominal stability of the real-time iteration scheme for nonlinear model predictive control".
- [17] Diehl, M., Bock, H. G., and Schlöder, J. P., 2005. "A real-time iteration scheme for nonlinear optimization in optimal feedback control". *SIAM J. control and optimization*, *43*(5), pp. 1714–1736.
- [18] Kirches, C., Wirsching, L., Bock, H., and Schlöder, J., 2012. "Efficient direct multiple shooting for nonlinear model predictive control on long horizons". *J. Process Control*, 22(3), pp. 540–550.
- [19] Andersson, J., 2013. "A General-Purpose Software Framework for Dynamic Optimization". PhD thesis, Arenberg Doctoral School, KU Leuven, Dept. of Electrical Eng. (ESAT/SCD) and Optimization in Eng. Center, Kasteelpark Arenberg 10, 3001-Heverlee, Belgium.
- [20] Ariens, D., Houska, B., Ferreau, H., and Logist, F., 2010. *ACADO for Matlab User's Manual*, 1.0beta ed. Optimization in Eng. Center (OPTEC), May. http://www.acadotoolkit.org/.
- [21] Mattingley, J., and Boyd, S., 2012. "Cvxgen: A code generator for embedded convex optimization". *Optimization and Eng.*, *13*(1), pp. 1–27.
- [22] Ferreau, H., Kirches, C., Potschka, A., Bock, H., and Diehl, M., 2014. "qpOASES: A parametric active-set algorithm for quadratic programming". *Mathematical Programming Computation*, **6**(4), pp. 327–363.
- [23] Binder, B., Kufoalor, D., and Johansen, T., 2015. "Scalability of qp solvers for embedded model predictive control applied to a subsea petroleum production system". In 2015 IEEE Conf. on Control Applications (CCA), pp. 1173–

- 1178.
- [24] Feyrer, K., 2007. Wire ropes. Springer.
- [25] Todd, M., Vohra, S., and Leban, F., 1997. "Dynamical measurements of ship crane load pendulation". In OCEANS'97. MTS/IEEE Conf. Proc., Vol. 2, IEEE, pp. 1230–1236.
- [26] Det Norske Veritas, A., 2014. "Environmental conditions and environmental loads".
- [27] Bock, H. G., and Plitt, K.-J., 1984. "A multiple shooting algorithm for direct solution of optimal control problems". Proce. the IFAC World Cong.
- [28] Wächter, A., 2009. "Short tutorial: getting started with ipopt in 90 minutes". In Dagstuhl Seminar Proc., Schloss Dagstuhl-Leibniz-Zentrum für Informatik.
- [29] Johansen, T. A., 2011. "Introduction to nonlinear model predictive control and moving horizon estimation". *Selected Topics on Constrained and Nonlinear Control*(1), pp. 1–53.
- [30] Vukov, M., Domahidi, A., Ferreau, H. J., Morari, M., and Diehl, M., 2013. "Auto-generated algorithms for nonlinear model predictive control on long and on short horizons". In 52nd IEEE Conf. on Decision and Control, IEEE, pp. 5113–5118.
- [31] Quirynen, R., Vukov, M., Zanon, M., and Diehl, M., 2015. "Autogenerating microsecond solvers for nonlinear mpc: A tutorial using acado integrators". *Optimal Control Applications and Methods*, **36**(5), pp. 685–704.